Journal of Medical Engineering & Technology, 2010; Early Online, 1–14

Innovation

Estimating the probability that the Taser® directly causes human ventricular fibrillation

H. SUN†, D. HAEMMERICH‡, P. S. RAHKO§ and J. G. WEBSTER*¶

†Department of Electrical and Computer Engineering, 1415 Engineering Drive, University of Wisconsin, Madison, WI 53706, USA
‡Division of Pediatric Cardiology, Medical University of South Carolina, 135 Rutledge Avenue, Charleston, SC 29425 USA
§Department of Medicine, University of Wisconsin, 600 Highland Ave Madison, WI 53792, USA
¶Department of Biomedical Engineering, University of Wisconsin, 1550 Engineering Drive, Madison, WI 53706 USA

(*Received 20 March 2009; accepted 23 November 2009*)

This paper describes the first methodology and results for estimating the order of probability for Tasers® directly causing human ventricular fibrillation (VF). The probability of an X26 Taser® causing human VF was estimated using: (1) current density near the human heart estimated by using 3D finite-element (FE) models; (2) prior data of the maximum dart-to-heart distances that caused VF in pigs; (3) minimum skin-to-heart distances measured in erect humans by echocardiography; and (4) dart landing distribution estimated from police reports. The estimated mean probability of human VF was 0.001 for data from a pig having a chest wall resected to the ribs and 0.000006 for data from a pig with no resection when inserting a blunt probe. The VF probability for a given dart location decreased with the dart-to-heart horizontal distance (radius) on the skin surface.

Keywords: Finite-element method; Cardiac stimulation; Electromuscular incapacitating device; Electrical safety; Taser®; Simulation

1. Introduction

The Taser® was designed to electrically stimulate skeletal muscles in order to incapacitate offenders so they can be apprehended [1] and is currently in use by law enforcement. During training, police officers are Tasered in the back, which does not cause ventricular fibrillation (VF). In contrast, offenders may be Tasered over the heart, which may cause VF. However many deaths following Taser® use may be caused by drug overdose, positional asphyxia, or other causes. This study focuses on determining whether VF can be directly caused by Taser® use. The Taser® impulses occur about 20 times per second for 5 s. The vulnerable period during the T wave will be hit for every heart beat.

It is difficult to achieve sustained VF in small hearts. Geddes [2] found the minimum cardiac critical mass for sustained VF was 18 g. Malkin *et al*. [3] found 7 g guinea pig hearts could consistently sustain tachyarrhythmias only when preceded by a rapid pacing protocol. Malkin and de Jongh Curry [4] found 7 g guinea pig hearts and 1 ms rectangular pulses from 10 to 160 Hz induced VF sustained for at least 10 s. Holden *et al*. [5] applied simulated M26 and X26 Taser® waveforms to the ventricular epicardial surface of guinea pig isolated spontaneously beating 3 g hearts using a 6 × 3 mm electrode, and were unable to

*Corresponding author. Email: webster@engr.wisc.edu

Journal of Medical Engineering & Technology
ISSN 0309-1902 print/ISSN 1464-522X online © 2010 Informa UK Ltd.
http://www.informaworld.com/journals
DOI: 10.3109/03091900903509149

induce VF. They increased the X26 Taser® waveform more than 240-fold higher than current densities predicted from their modelling and were unable to induce VF. They concluded 'a lack of arrhythmogenic action of the M26 and X26 Taser device'. Thus Tasers® have never caused VF in small hearts. However Tasers® have caused VF in the much larger live pig hearts [6–8]. The similarities between this study and that of Holden *et al*. [5] are that we both used electromagnetic modelling of the human. However, our study used actual X26 waveforms to actual 9 mm electrodes in intact live pigs with 400 g hearts, which correspond most closely with live humans, and achieved sustained VF, whereas Holden *et al*. [5] were unable to achieve VF with simulated X26 waveforms.

This study was designed to determine the mean of probability of Tasers® (model X26) causing VF in humans through electrical stimulation, using (1) computer models, (2) data on dart-to-heart distances that caused VF from two pig studies, (3) human skin-to-heart minimum distances measured using echocardiography, and (4) data on Taser® dart landing statistics from police reports [1].

2. Methods and examples

This study examined the Taser® model X26, so in the following sections we will refer to this model as 'Taser'. By 'VF distance' we mean the maximum distance between Taser dart tip and heart at which VF can be induced. VF distance is the same as 'dart-to-heart VF distance'. 'VF skin-to-heart distance' indicates the VF distance plus the dart length inside the skin.

Two sets of sedated pig study results were used. In one study, the pig chest wall was resected and a sharp dart approached the heart [9]. In a second study, a blunt dart was inserted from the pig's skin [10]. The dart was blunt to ensure it does not puncture the heart.

Cell stimulation strength–duration curves derived from the resistor–capacitor (*R–C*) cell-membrane models show that the cell stimulation caused by short duration electric pulses is governed by the charge. At the surface of the heart, for the short duration pulses of Tasers, charge density or the electric field/duration time threshold causes excitation [11]. Our key strategy to solve the problem was to estimate the area of the chest skin surface where, if a Taser lands, VF will likely ensue. This area was determined by whether the charge density induced on any point of the heart exceeds the VF threshold charge density. The area is a function of the minimum skin-to-heart distance (given by human echocardiography experiments), the shape of the human torso and heart geometry (using a typical geometry) [12,13], the length of the dart (measured fixed length), the charge from the dart (constant for Tasers of the same type), the assumption about how close the dart tip has to be in order to cause VF (measured by pig experiments) and the VF threshold of human heart stimulation. Once known, this area can be multiplied by the known likelihood of a dart hitting that area (which is calculated from police data).

To estimate the surface area given one human geometry, all the above conditions are known except the VF threshold of human heart stimulation. The human VF threshold for short-duration electrical stimulation is not available in the literature. Our pig experiments measured VF distances but the charge density VF thresholds could not be measured. Therefore pig VF distances were used to derive internal VF thresholds using our finite element (FE) computer models.

For the same current waveform with the same duration, that is, same charge, current density per unit inserted current can be used as the internal VF threshold. The charge density is defined as charge per unit area and charge density is the integration of the current density over time. Since current density scales linearly with total injected current and it is assumed charge density scales linearly with the total charge in the same proportion, the charge density is only related to the total charge and the current density per unit inserted current. Since we care about charge density only, and the total charge is the same for the same Taser, the charge was not needed. Charge is only useful when extending the X26 results to other types of EMDs. Therefore the current density values for 1 A inserted current were calculated in our FE models.

Current density can be directly calculated by our electrostatic FE models since the problem could be approximated as an electrostatic problem in the Taser's operating spectrum. The quasi-electrostatic hypothesis was studied in chapter 2 of [14].

Thus, internal human VF current density thresholds were first derived using the current density values per unit inserted current at distances from the skin that equalled the pig experiment VF distances caused by a Taser dart placed at similar settings of pig experiments (between ribs) using 3D FE models. In these models we assume that dart-to-heart VF distances are the same in pigs and humans.

Such internal VF thresholds calculated by FE models are useful to derive the VF stimulation area on the skin surface. All current density values are computed for a 1 A inserted current and dart placement is moved on the skin surface with respect to the heart.

Three factors on which VF depends are VF thresholds, human anatomies and dart landing locations. Different pigs have different VF thresholds. Different humans also have different VF thresholds, as well as having different skin-to-heart distances. To estimate the probability of VF, we need to combine information from humans, pigs and dart locations. However, an atlas of anatomy data for all sizes of humans was not available.

We modelled the differences in humans by using data of the minimum skin-to-heart distances measured by echocardiography. A fixed torso anatomy had a global coordinate system noted as x', y', z' assuming one typical human heart and ribs anatomy. A movable local

coordinate system noted as x, y, z permitted the FE model dart to move around relative to the heart of the fixed global coordinate system (figure 1). A local system with limited geometry size also allowed fine FE meshes. The current density values at the heart for different dart locations and heart depths were compared to the internal VF thresholds to determine whether or not VF could occur.

Contours on planes parallel to the skin were deployed to simplify the process so the problem can be solved by checking a series of heart slice contours and current density contours on these planes. A human heart geometrical model [13] was sliced to show heart boundary contours on planes parallel to the front skin. Ribs were projected to determine which electric current density contours should be used when moving the dart—the contours for a dart between ribs or a dart on top of ribs or touching ribs. Current density contours with the internal VF threshold values were determined on the same planes, and were generated for different dart locations relative to ribs (between ribs, on top of ribs or sternum). We determined the area where VF could be induced if the dart lands in this location by moving a dart on the torso skin and comparing the current density values inside the heart with internal VF threshold values on all planes parallel to the skin. If the electric current density contour on a plane caused by the dart intersects the heart slice on the same plane, the dart lands in an area where VF will be caused. Details will follow in §2.2.1.

Finally, dart landing statistics were included to calculate the mean and variance of the total probability of VF. From the equivalent dart area where VF will be caused, we derived the mean and variance of the conditional probability of VF given a dart location on the skin and the dart location radii where VF will be caused.

For the convenience of illustrating the process, a list of variables shown in figure 2 follows. Variables starting with y are distances along the y axis in the local coordinate system, which is perpendicular to the skin. In the variable subscript, 'd' indicates 'dart', 'h' indicates 'heart', 's' indicates 'skin', 'c' indicates 'contour', 'min' indicates 'minimum', and 'VF' indicates 'ventricular fibrillation'.

- y_{dh_VF} (mm): Dart-to-heart distance that caused VF in pig experiments [9,10] where a dart was inserted between ribs. We assume humans have the same VF distance as pigs.
- y_{sh_VF} (mm): y_{dh_VF} + dart length. Skin-to-heart distance that caused VF in pig experiments, for a dart inserted between ribs, which follows $y_{sh\_VF} = y_{dh\_VF} + 9$ (mm).
- y_{sh_min} (mm): Minimum human skin-to-heart distances considered for a given VF skin-to-heart distance y_{sh_VF}, which follows the relation that $10 \le y_{sh\_min} \le y_{sh\_VF}$ (mm).

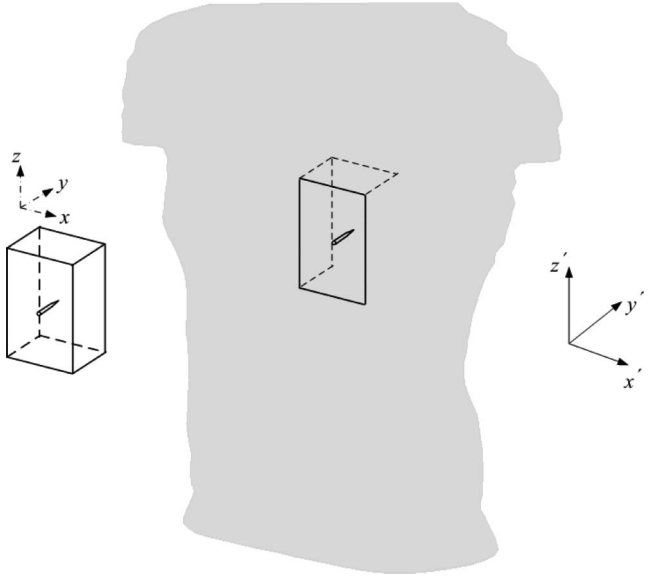

Figure 1. The general model with two coordinate systems. The x, y, z coordinate system is the local coordinate system for each dart location with the centre of the dart-skin interface as the origin. The x', y', z' coordinate system is the global coordinate system for the torso.

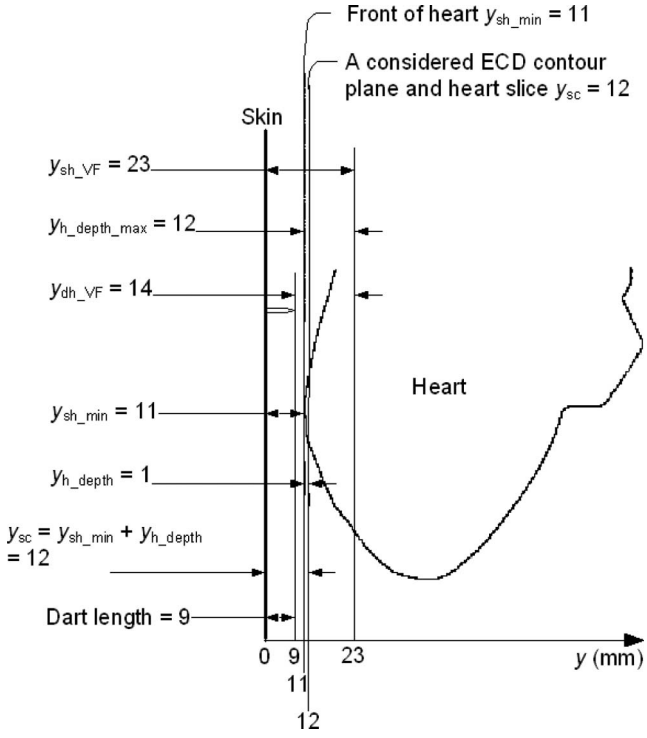

Figure 2. Side view of skin, heart slices, and electric current density contour planes. One plane is 12 mm away from the skin. The deepest plane considered is 23 mm away from the skin if the VF skin-to-heart distance is 23 mm. All distances are in mm, using the local coordinate system.

- $N\_y_{sh\_min}$: Number of humans with minimum skin-to-heart distances in the 1 mm bin $[y_{sh\_min}-1,\ y_{sh\_min}]$ (mm) from echocardiography data.
- $P\_y_{sh\_min}$: Probability of humans in the bin $(y_{sh\_min}-1,\ y_{sh\_min})$, which is estimated as $N\_y_{sh\_min}$ divided by total number of humans (150) in the echocardiography data.
- y_{sc} (mm): Skin-to-contour locations of electric current density contour planes considered (distances from the skin) in the y-direction, which follow the constraint that $y_{sh\_min} \le y_{sc} \le y_{sh\_VF}$. Because only the electric current density contour planes that could intersect a heart slice and could have larger current density than the VF threshold, that is, closer to the skin than the VF skin-to-heart distance y_{sh_VF} needed to be considered. $y_{sc} = y_{sh\_min} + y_{h\_depth}$.
- y_{h_depth} (mm): Human heart slice depths (distance of a heart slice to the front of the heart), which follow the relation that $y_{h\_depth} = y_{sc} - y_{sh\_min}$ (mm). So $0 \le y_{h\_depth} \le y_{h\_depth\_max} = (y_{sh\_VF} - y_{sh\_min})$ (mm). For example, the slice at the depth $y_{h\_depth} = 0$ mm was roughly just one point. Since $0 \le y_{sh\_VF} \le 33$ mm, 10 mm $\le y_{sh\_min} \le y_{sh\_VF}$, $0 \le y_{sh\_VF} - y_{sh\_min} \le 23$ mm, the deepest heart slice $y_{h\_depth\_max}$ that needed to be considered was 23 mm.
- $A\_y_{sh\_min}\_y_{dh\_VF}$ (cm^2): Area where the dart caused current density at any point of heart > VF threshold) for a given minimum skin-to-heart distance y_{sh_min} (mm) and a given VF dart-to-heart distance y_{dh_VF} (mm). This area was the union of the locations causing VF for all heart slices under consideration.
- $P\_hitting1cm^2\_y_{sh\_min}$: The probability of a hit in 1 cm^2 in B3 and C3 grids [8] on the front chest for this group of subjects with given minimum skin-to-heart distances in the bin $(y_{sh\_min}-1,\ y_{sh\_min})$.
- $P^{VF}\_y_{sh\_min}$: Probability of human VF for this group of subjects with given minimum human skin-to-heart distance in the bin $(y_{sh\_min}-1,\ y_{sh\_min})$, which follows the equation that $P^{VF}\_y_{sh\_min} = A\_y_{sh\_min}\_y_{dh\_VF}$ (cm^2) $\times$ $P\_hitting1cm^2$.

The following subsections give further details.

2.1. FE modelling

In order to compute the probability of the Taser electrically inducing human VF, different human heart locations and different dart locations would usually require different geometrical models. If a single mesh representing one person's anatomy or dart location were created for each combination, the calculation times would have been prohibitively long. Instead a simplified general model was designed to make the work solvable. That is, a fine mesh FE model was created only around a dart including a small and reasonable region where the dart could cause VF. By 'general', we mean we did not create multiple FE models for all combinations of heart locations and dart locations. A simplified general model was created for each dart/human interaction scenario (arcing though the air to one point on the skin, a dart inserted between ribs, on top of ribs), by virtue of the following attributes and assumptions of the problem:

(1) The 9-mm dart penetrates the skin by 9 mm if between the ribs, or hits the ribs with a shorter penetration depth of 5 mm, or the Taser electrically arcs through the air to a single point on the skin.
(2) The current density decreases dramatically with distance away from the dart.
(3) To determine VF only the current density at the heart is of interest.
(4) From VF distances in pig data [9,10], only thin humans with a short dart-to-heart distance need to be considered as we did not find VF induced above a certain dart-to-heart distance.
(5) Similarly, the short dart-to-heart distances required for VF necessitate the dart being over the heart. Tissues in this domain such as intercostal muscle, heart and blood have roughly similar conductivities except for the ribs and sternum.
(6) Lungs were not included in the model between the dart and heart due to modelling the worst-case considerations: lungs are usually not on the shortest path between the skin and the heart, as shown in [10]. Deflated lungs at the end of expiration have similar conductivity as muscle and inflated lungs would cause lower current density in the heart. If you are thin and put your fingers between your ribs right over your heart (at the point of maximum impulse) you can feel your heart beating right on the other side of your ribs during the portion of the breathing cycle when the lungs are deflated. The 9-mm dart of a Taser can easily penetrate the skin, 5 mm of fat into the intercostals muscle and get within 2 mm of the heart. Hence we assume lack of skin, fat and lung tissue.

The current density values for a 1 A inserted current at the same dart-to-heart distance and for approximately the same dart placement as in the pig experiments [9] (sharp dart inserted between ribs) generated internal VF threshold current density values. The FE modelling results showed that the difference of the current density values at the heart locations caused by blunt and sharp darts could be ignored. Thus the internal VF threshold current densities for VF distances for pig data using a blunt dart [14] used the sharp dart in the FE modelling.

For other dart placements (on top of ribs or sternums), the FE models were used to calculate the current density while keeping the injected current constant. For a human with different anatomy, characterized by the minimum skin-to-heart distance, the current density values at

different skin-to-heart distances could be derived from the same model without creating new FE geometry for new anatomy due to attributes (1)–(6) above.

2.1.1. Software and hardware. ABAQUS 6.5 (ABAQUS, Providence, RI, USA) was used to solve the FE model for current density. MSC PATRAN 2005 (MSC Software Corporation, Santa Ana, CA, USA) was used to generate the geometry and generated the mesh input file for ABAQUS. MATLAB 7.4 was used to preprocess and postprocess the input and output data for ABAQUS. Each ABAQUS model was run on a computer with Linux operating system. It required 3 GB of memory, at least 4.08 GB hard drive allocated for generated files, and took about 1.5 h with an additional 0.5 h for postprocessing using MATLAB. Each PATRAN model was run on a Sun Blade 1000 computer with a UNIX operating system that had a 2.5 GB memory, and took about 3 h [14].

2.1.2. Geometry modelling. FE models with simplified geometry were created using the PATRAN software. FE models of a box size of $60 \times 40 \times 60$ mm with one dart inserted in the centre of the skin surface and other surfaces grounded were designed to compute current densities between the dart and human heart.

The VF dart-to-heart distances from pig experiments ranged from 0 to 24 mm and had a 2 mm resolution. For the 9-mm long dart, the human VF skin-to-heart distances would range from 9 to 33 mm. Thus only heart slices located less than 33 mm deep from the skin had to be considered to match the pig experimental data. The current density decreased dramatically away from the dart tip, so placing the current sink depth at 40 mm was satisfactory for a human torso thickness of about 180 mm.

Two dart types were modelled, both with a diameter of 0.8 mm and length of 9 mm. The sharp dart with omitted barb was modelled as a cylinder of 6 mm abutted to a cone of 3 mm for all results in this paper, unless specifically labelled blunt. We assumed the barb does not make a significant difference to current density at the heart and it was omitted for simplicity. The tip-less blunt dart was modelled as a 9-mm long cylinder. An electric arc passing from the dart though clothing to the skin was modelled with the current injected at a single point on the skin.

A source voltage (+5 V) was assigned to the dart surface, or to one mesh node when an electric arc was simulated. A sink voltage (–5 V) was assigned to the five surfaces other than the skin. While Taser devices have two darts, we used only a single dart in the models because in preliminary models we found similar current density values around a single dart model as in two-dart models due to the large distance (>16 cm) between the darts. The resulting current densities in the model were scaled such that the total inserted current was 1 A.

The size of two ribs was determined by measuring the rib cross section in figure 4 of [15]. The ribs were modelled as elliptical cylinders 5 mm below the skin with a width of 12 mm, a thickness of 5.12 mm, a length of 60 mm and a separation of 18 mm. The rest of the box outside of the elliptical cylinders was assumed to be muscle. The sternum was modelled as an elliptical cylinder with a width of 30 mm [16], a thickness of 10 mm [17] with the same conductivity as bone. All the elliptical cylinders in the model had a length of 60 mm which was the same as the box. The models for the situations when the dart was inserted between ribs, touching one rib, on top of one rib (the length of dart penetration was only 5 mm) and at a single point on the skin were created in PATRAN.

2.1.3. Mesh generation and tissue properties. The dominant tissues between skin and heart are muscle and cartilage. Far away from the sternum the ribs are bone with low conductivity. Near the sternum over the heart the ribs consist of cartilage with medium conductivity for people below 35 years of age, and of bone with low conductivity for people older than 35 years. By setting the conductivity of the two ribs the same as bone, a new model for ribs was obtained, and another model without ribs or cartilage was obtained by setting the conductivity of the two ribs the same as muscle. Comparison of ribs, cartilage or muscle was conducted for a dart inserted between ribs.

All tissues were treated as isotropic. We did not model the anisotropic characteristics of the bidomain model because of computer limitations. Ribs had conductivities for bone or cartilage while all other tissues had conductivities of muscle. Table 1 provides the number of tetrahedral elements and the conductivity of each tissue. The conductivity values were based on the frequency-dependent tissue conductivity model developed by Gabriel *et al*. [18]. A frequency of 5 kHz was chosen since it is the first dominant peak of the X26 power density spectrum [14]. A tetrahedron element type was chosen since its shape was suitable to generate a quality mesh for geometry with curvatures such as darts and ribs in our application. We used a global element edge length of 1 mm for non-rib parts. The accuracy of FE models with tetrahedral elements of a global edge length of 1 mm was validated by a convergence test and by comparing results with those obtained by other methods, such as analytical equations. The element size was small enough so that the 2-mm resolution pig experimental data could be used effectively, but not so small that there were too many elements to permit ABAQUS to solve the problem.

2.2. VF probability calculation

2.2.1. Determining dart locations where VF will be caused. For a given person (the minimum skin-to-heart distance y_{sh_min} and VF threshold) and given dart location and given

Taser, the VF probability was either 1 or 0. Heart and ribs anatomy and current density contours around a dart with the values of the internal VF thresholds were considered together to determine the dart locations where VF will be caused.

The minimum skin-to-heart distances y_{sh_min} for standing humans measured from echocardiography in the Adult Echocardiography Laboratory at the University of Wisconsin Hospital and Clinics were used to characterize variations of human anatomy [14,19]. The studies were performed on standard ultrasound equipment manufactured by Philips Medical Systems (Andover, MA, USA), Siemens Acuson (Malvern, PA, USA), or General Electric (Waukesha, WI, USA). Standard adult transducers were used. Transducers were evaluated to check for accuracy of the measurement capability of the systems using standard phantoms. 2D echocardiograms were performed in 150 consecutive adults. Three views were obtained, the first being the best possible parasternal (sternal border) long axis (vertical) view of the heart, the second being the best apical (tip) four-chamber view of the heart and the third being the best subcostal (under ribs) four-chamber view. For each imaging location an average of 10 beats were obtained during quiet respiration. After the recordings of the images in the subjects were made, the information was downloaded into a Camtronics Workstation. Images were analysed to determine the shortest linear distance from sector origin (skin surface) to epicardial surface. Using the analysis package on the workstation, the workstation was calibrated, and the calibration marks on the ultrasound loop for each measurement were made. Data were mean $\pm$ standard deviation (SD), analysed by ANOVA.

The other parts of human anatomy used a typical anatomy of the heart and ribs. To create a typical anatomy, the Utah ribs [12] and Texas heart [13] (figures 3–6) were combined by rescaling and translating the Texas heart mesh. The relative location of the heart to ribs in x' and z' directions was verified by checking with anatomy experts and references [20]. The relative distance of the heart from the front of skin in the y' direction was not considered, since later the heart was placed at different y distances according to the echocardiography data, and current density in the heart for that heart location was determined. Since the x'–z' plane (chest frontal plane) differs from the x–z plane where the dart was inserted in the FE model, the anatomy geometry was rotated to align the chest frontal surface x'–z' plane with the FE model x–z plane.

The current density values at the locations corresponding to the VF distances away from the skin on the axis perpendicular to the skin caused by a sharp dart inserted between two ribs made of cartilage were used as the internal current density VF thresholds for all VF distances measured from the pig experiments. The contours of electric current density caused by a dart on planes parallel to the skin and contours of heart slices parallel to the skin were generated. The electric current density contours for the dart between the ribs and hitting the ribs were used to calculate the probability of VF. The dart touching the rib was similar to between the ribs as shown in [14], so these were combined. Thus the current density contour for a dart between the ribs was used for the dart touching the ribs.

For a specific dart location, when any heart boundary contour at any depth y_{h_depth} intersected with the current density contour with the value of the internal VF threshold on that plane y_{sc} ($= y_{sh\_min} + y_{h\_depth}$), it was assumed that VF occurs, given that VF threshold. This contour examination was performed for planes at distances $y_{sc} = y_{h\_depth} + y_{sh\_min}$ from the skin. The dart was moved around on the skin surface to derive the area where VF will be caused for the given heart location. Convolving the current density contour with the internal VF threshold value corresponding to a given VF distance and the heart slice area on the same plane, parallel to the skin, results in the dart area where VF will be caused for that plane, given the VF distance. Both heart boundary contours and current density contours were approximated as circles. Then, the dart area where VF will be caused considering a certain plane parallel to the skin was estimated as a circle with a radius of the sum of the radii of the heart slice and the electric current density contour, with the value of the internal VF threshold on the same heart slice caused by the dart placed on the skin (figure 3).

For the locations where ribs were above the heart, the current density contours for a dart hitting ribs were used.

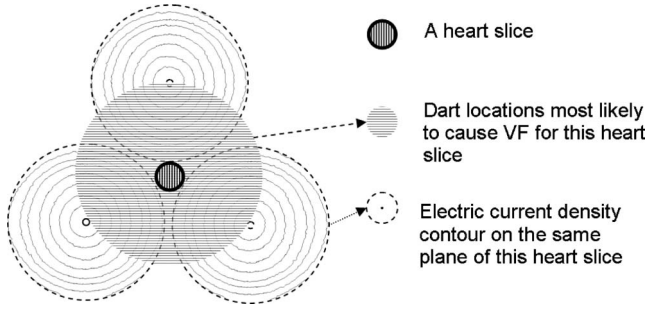

Figure 3. Dart location area (at the skin) most likely to cause VF for a heart slice (at a given depth below the horizontal striped circle) is estimated as a horizontal striped circle with a radius of the sum of (1) the heart slice radius (vertical striped circle) and (2) the electric current density contour (dashed line circumference) on the heart slice caused by the dart placed on the skin. For the heart locations (less than 33 mm from the skin), heart slices closer to skin have a smaller radius but have a larger current density contour. So all heart slices for one given heart location must be checked to determine a maximum of the sum of the heart slice radius and the electric current density contour on the heart slice caused by the dart placed on the skin.

Table 1. Description of the models.

Tissue	Number of tetrahedrons	Global edge length (GEL)	Minimum edge length	Conductivity (S m^{-1}) at 5 kHz
Two elliptical ribs	56 842†	4.7 mm	GEL × 0.1	0.17552 (cartilage)
	58 083‡	4.7 mm	GEL × 0.1	0.020346 (rib)
	59 119§	4.7 mm	GEL × 0.1	0.33653 (muscle)
Other parts in the box	1 177 199†	1 mm	GEL × 0.2	0.33653 (muscle)
	1 168 989‡	1 mm	GEL × 0.2	0.33653 (muscle)
	1 128 226§	1 mm	GEL × 0.2	0.33653 (muscle)

†The model has a sharp dart with 0.8 mm diameter.
‡The model has a blunt dart with 0.8 mm diameter.
§The model has one node electric source as arc of dart.

For the locations where the heart was exposed without ribs, the current density contours for a dart inserted between the ribs were used.

The overall dart area where VF will be caused for a person with a heart at a given minimum skin-to-heart distance y_{sh_min} (i.e. measured at the location where the heart is closest to the skin) using a certain VF distance y_{dh_VF} from pig data was estimated by the union of the dart areas where VF will be caused if a dart hits within that area, considering all planes of the heart parallel to the skin deducting the sternum area, where a dart will not penetrate near the heart. Assuming the circles on different planes are concentric, the largest radius where VF will be caused over all planes corresponded to the union of all heart slices for each heart location. For the heart locations we were interested in (less than 33 mm from the skin), when the heart slice radius increases, the electric current density contour on the heart slice decreases. So the sum of the two does not have a monotonic trend. Therefore we examined all the heart planes/slices to determine a maximum size of the radius where VF will be caused. Such procedures were then repeated for each VF distance from the pig datasets.

To illustrate how to determine dart locations where VF will be caused for a given VF distance threshold and human heart location, we give an example using some figures that would normally appear in the results section. The following example is for a dart-to-heart VF distance y_{dh_VF} of 14 mm and a person with minimum skin-to-heart distance y_{sh_min} of 11 mm.

First using the FE model shown in figure 4, the current density values at these locations corresponding to VF distances on the y-axis (dart direction) for the dart inserted between the ribs were found using interpolated current density values on the y axis for the dart-to-heart distances y_{dh_VF} of 0, 2, 4, 6, …, 24 mm, or $y_{sh\_VF} = 9, 11, 13, 15, \ldots,$ 33 mm. These yielded the internal VF threshold current density values (figure 5). For a given dart-to-heart VF distance of $y_{dh\_VF} = 14$ mm, the VF skin-to-heart distance would be $y_{sh\_VF} = y_{dh\_VF} + 9 = 14 + 9 = 23$ mm. The current density along the y-axis at $y = 23$ mm was 358 A m^{-2}, according to figure 5. Therefore, 358 A m^{-2} was used as the internal VF threshold current density for the pig data that caused VF on the heart 14 mm from the dart tip.

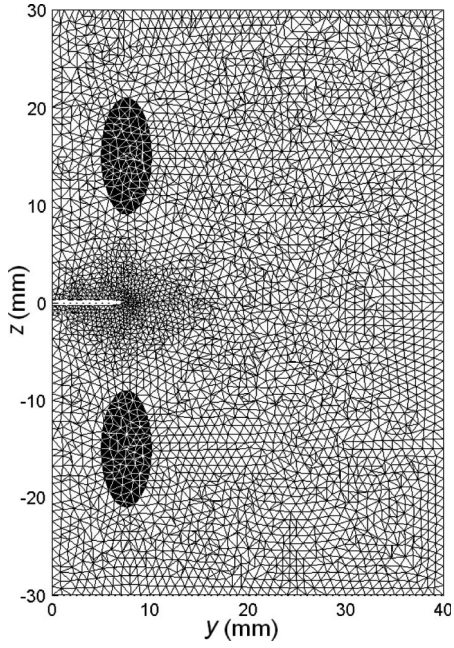

Figure 4. The cut view of the mesh from the 60 × 40 × 60 mm FE model for the sharp dart of 0.8 mm diameter on the plane of $x = 0$ shows a 9 mm dart between two 5 × 12 mm elliptical ribs spaced 18 mm apart and 5 mm away from skin.

For each pig VF skin-to-heart distance of y_{sh_VF} (mm), the humans with their hearts located at various minimum human skin-to-heart distances y_{sh_min} based on echocardiography data were studied. The considered y_{sh_min} for a given y_{sh_VF} follows $10\text{ mm} \le y_{sh\_min} \le y_{sh\_VF}$, where 10 mm is the shortest distance from echocardiography. For each person with the heart front located at y_{sh_min}, only heart slices at depths less than or equal to the VF skin-to-heart distance y_{sh_VF} needed to be considered, since from the pig data no VF occurs at larger depths. This example used the pig VF skin-to-heart distance of $y_{sh\_VF} = 23$ mm, so the minimum human skin-to-heart distances considered were larger than 10 mm and smaller than the VF skin-to-heart distance y_{sh_VF} of 23 mm. Also a minimum human skin-to-heart distance of 11 mm lies in the range of [10 mm, 23 mm]. For this distance of 11 mm along the y-axis from

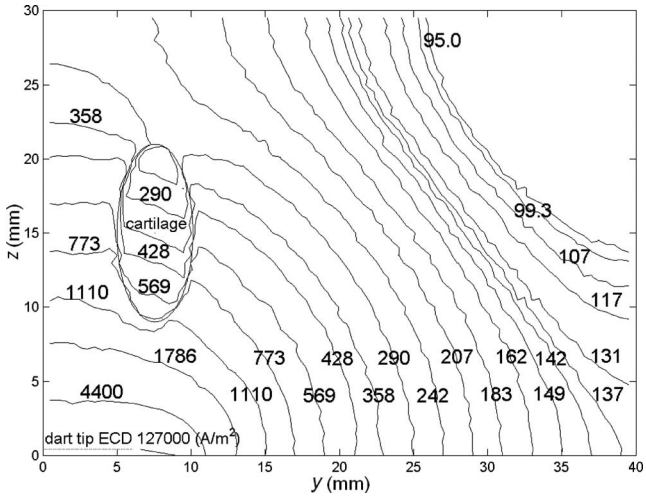

Figure 5. For a 1-A inserted current, the contour lines of current density (A m^{-2}) on the plane of $x = 0$ for a sharp 0.8 mm dart. The current density values along the dart direction (y) pointed toward the heart will be used as the internal VF threshold current density values for the corresponding VF distances. Current density numbers have three significant digits. All distances are in mm, using the local coordinate system.

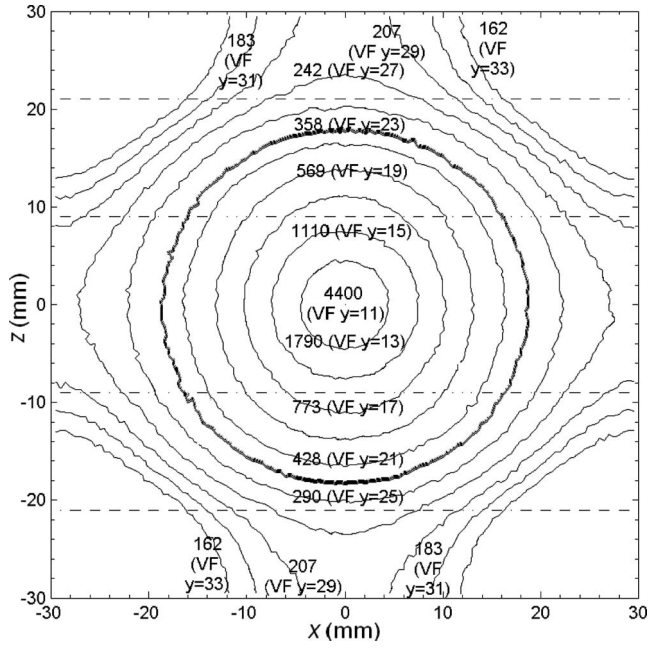

Figure 6. For a 1-A inserted current, the contour lines of current density (A m^{-2}) on the plane of $y = 11$ mm for a sharp dart inserted between two cartilage ribs (two pairs of dotted lines). VF $y = ?$ (where ? is the number shown) by each contour line labels the VF distance plus dart length (9 mm) predetermined from figure 5 for the internal VF threshold with the current density value of that contour line in figure 6. So each contour line in figure 6 encircles an area subject to VF when a dart lands at the origin ($x = 0$, $z = 0$) and between ribs, for the labelled VF $y = ?$. Current density numbers have three significant digits.

the skin to the front of the heart, we needed to decide how many heart slices needed to be considered. The deepest considered heart slice in this example was located at the VF skin-to-heart distance y_{sh_VF} from the pig data used, that is, 23 mm. The depth relative to the front of the heart for the heart slice was labelled on the heart contour map (figure 7). The depth of the heart slice was simply the distance of the heart slice to the front of the heart. The depth of the deepest considered heart slice was the y-axis location of the deepest heart slice minus the y-axis location of the front of the heart: $y_{h\_depth\_max} = y_{sh\_VF} - y_{sh\_min} = 23 - 11 = 12$ mm (figures 2, 7). Therefore the relevant heart slices considered were at depths of $0 \le y_{h\_depth} \le y_{h\_depth\_max} = 12$ mm. The equivalent radii of the heart boundary contours were estimated by the distances between the contours and the origin on the diagonal lines of the contour squares.

We needed to consider current density contours and heart slices on a series of planes located at y-axis coordinates y_{sc}, where $y_{sh\_min} \le y_{sc} \le y_{sh\_VF}$. In this example, 11 mm $\le y_{sc} \le$ 23 mm.

First we looked at a specific plane $y_{sc} = 23$ mm. The current density contours on the $y = 23$ mm plane for a dart inserted between the ribs is shown in figure 6. In figure 6, we looked for the current density contour with the value of the internal VF threshold 358 A m^{-2} determined from figure 5. It had a radius of about 18 mm. Since the front of the heart was at $y = 11$ mm, the heart slice depth on this plane for this person was 23 mm – 11 mm = 12 mm. From the overlaid graph of ribs and heart slices (figure 7), the heart slice at that slice depth 12 mm had a radius of about 33 mm in chapter 4, table 1 of [14]. The dart area where VF will be caused on the skin surface for this heart slice in this example was estimated to have a radius of 33 mm + 18 mm = 51 mm, if using the contour for a dart between ribs.

Then we examined all planes considered. In this example, minimum skin-to-heart distance y_{sh_min} was 11 mm; these planes were at distances [11 mm, ..., 23 mm] from the skin as shown in table 2.

2.2.2. Mean estimation of VF probability. After determining dart locations where VF will be caused for all relevant human minimum skin-to-heart distances and pig VF distances, the total probability of Tasers directly causing VF in humans was estimated by combining these data with the dart landing probability distribution in table B-1 of [1]. The probability of a hit in 1 cm^2 in the frontal chest area for each group of human minimum skin-to-heart distances ($P\_hitting1cm^2\_y_{sh\_min}$) was calculated [9,10] using dart landing data and human height of the group. Multiplying this probability by the dart location area (in cm^2) where VF will be caused for the same group

($A\_y_{sh\_min}\_ y_{dh\_VF}$) yielded the human VF probability for this group $P^{VF}\_y_{sh\_min}$. The mean of the total VF probability was obtained by aggregating $P^{VF}\_y_{sh\_min}$ over all groups of human minimum skin-to-heart distances and pig data, assuming the dart landing locations, the pigs in the pig experiments and the humans in the echocardiography experiments were all independent with equal probability of occurrence, and assuming the human VF probability had same equal mean and variance as in data from each pig.

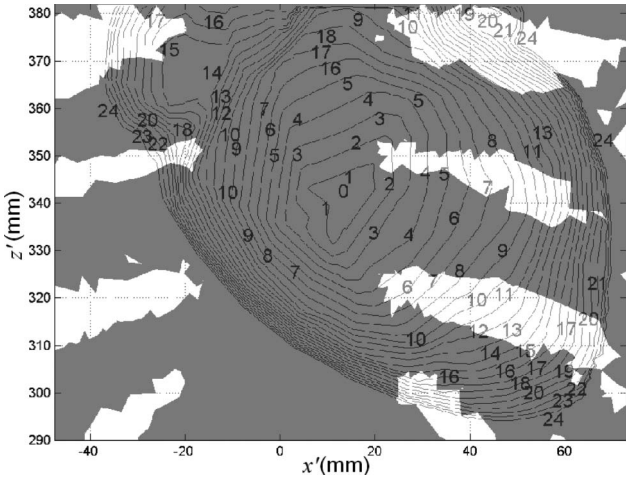

Figure 7. Contours of the rotated ventricle slices at depths 0 to 24 mm under rotated ribs. Values on the contours show the depths (distance to the plane closest to the rotated skin with the same rotated angle). The heart slice at depth i mm was labelled with i. Depth i corresponds to y_{h_depth} (column 4 in tables 2 and 3). The front view of the 0 mm depth heart slice closest to the skin shows that the closest place was on the right ventricle. Gray colour indicates the projected sternum and ribs. Axes use the global coordinate system, while heart depths are relative to the front of heart.

Conditional VF probability was estimated for each dart-to-heart radius (horizontal distance) on the frontal chest plane (i.e. a plane perpendicular to the dart insertion direction). The estimated conditional VF probability for a certain dart-to-heart radius is where the proportion of samples with a dart area radius is equal to or larger than that dart-to-heart radius. More details are given in §2.2.5.

2.2.3. Estimating the variance of the VF probability. There were three sources of variance for the VF probability: humans (echocardiography data for skin-to-heart distances), pigs (VF distance data) and dart hitting data. Briefly, pigs were assumed independent and each pig (not the VF threshold values provided by pigs) had equal probability. Humans were assumed independent and each human had equal probability. For given pig data, VF probability values for humans were assumed independent and had a same mean and variance. But human VF probability values for one pig datum may have different mean and variance from human VF probability values for another pig datum. The human VF probability values follow a mixture of the conditional distributions given each pig. Dart hittings provided a multiplier (proportion of hittings falling in B3 and C3 grids) when calculating probability values. The hitting proportion was assumed independent with pigs and humans. So the expectation of the product was the product of the expectations and the variance was also derived.

First the sample mean and sample variance of human VF probability, given each pig datum, were calculated. Then the sample means based on each pig datum were averaged to get the sample mean aggregated over all pigs and humans. The sample variances based on each pig datum

Table 2. Probability results based on pig data using blunt probe [19] of VF skin-to-heart distance $y_{sh\_VF} = 8 + 9 = 17$ mm), internal VF threshold current density = 773 A m^{-2} for 1 A inserted current.

y_{sh_min} (Min. skin to heart distances for the given VF dart-to-heart distance)	$P\_y_{sh\_min} = N\_y_{sh\_min}$ /150 (Fraction of population with min skin to heart distance y_{sh_min})	$y_{sc} = [y_{sh\_min}, y_{sh\_min} + 1, \ldots, y_{sh\_VF}]$ (Electric current density contour plane locations)	$y_{h\_depth} = y_{sc} - y_{sh\_min} =$ [0, 1, …, $y_{sh\_VF} - y_{sh\_min}$] (Heart slice depths)	$A\_y_{sh\_min}\_y_{dh\_VF}$ (cm^2) (Area where the dart was most likely to cause VF)	$P^{VF}\_y_{sh\_min} = A\_y_{sh\_min}\_y_{dh\_VF} \times P\_hitting1cm^2\_y_{sh\_min}$ (VF Probability for people with y_{sh_min})
17	0.0133	[17]	[0]	0	0
16	0.00667	[16, 17]	[0, 1]	0.00716	0.00000267
15	0				0
14	0				0
13	0.02	[13, …, 17]	[0, …, 4]	0.532	0.000204
12	0.00667	[12, …, 17]	[0, …, 5]	1.61	0.000583
11	0.00667	[11, …, 17]	[0, …, 6]	3.33	0.0012
10	0				0

The population VF probability estimated (by summing the products of columns 2 and 6) for pig data using a blunt probe VF dart-to-heart distance, y_{dh_VF}, of 8 mm is 0.0000161.

were averaged to get the sample variance aggregated over all pigs and humans.

The count of hits falling in B3 and C3 grids was assumed a binomial distribution. The mean of the proportion was estimated as the count of hits in B3 or C3 divided by the total count of hits. Then based on independence between hitting and humans or pigs, the variance of the product was derived.

2.2.5. Conditional VF probability as a function of dart-to-heart horizontal distance (radius). Intuitively, the closer the dart to the heart, the more likely VF would be caused. Although a dart on a circle with a certain radius from the heart could not cause VF if the dart were located on top of the sternum, in this process, the estimation of dart area radius most likely to cause VF was based on a situation where the dart does not land on the sternum. This will overestimate the conditional VF probability. But the goal of the paper is to study the total VF probability, not the conditional VF probability. It is more of interest to verify the relation between the conditional VF probability and the dart-to-heart radius.

The equivalent dart location radii (before considering the sternum) where VF would be caused were already calculated for each human and pig datum when calculating the total VF probability. Assuming the VF probabilities for each human datum and pig datum were independent with equal probability, for a certain dart-to-heart horizontal distance, the proportion of samples with a radius where VF would be caused equal or larger than that distance was the estimated VF probability for that distance. The distance most likely to cause VF would be the locations appearing most frequently.

Given a dart on a circle of a given radius r, reusing the symbols used in derivation for the dart hitting count in Appendix 2.2 in [14], assume a randomly-drawn sample of l samples were independent and have the same probability W of VF, then the count of VF in l trials, denoted by O, has a binomial distribution with parameters W and l.

$$E(O) = l\,W,\ \overline{Var(O)} = l\,W(1-W), \tag{1}$$

where O is the number of samples with radius where VF would be caused equal to or larger than r and $l = mn$.

$$\hat{W} = \frac{O}{l} \tag{2}$$

$$\hat{V}ar(\hat{W}) = \frac{\hat{W}(1-\hat{W})}{l}. \tag{3}$$

3. Results

3.1. FE model results

We created FE models using the geometry similar to figure 4 with (1) the dart inserted between the ribs; (2) the dart inserted touching the edge of one rib; (3) the dart inserted on the centre top of one rib; (4) the dart away from the skin with an electrical arc to skin, as a node on the skin between two ribs; (5) a node on the skin in front of one rib edge; and (6) a node on the skin in front of the centre of one rib. Here, we reduced these to three example categories and only present these: dart inserted 9 mm, dart inserted 5 mm, dart as a node. For a dart hitting the ribs, its maximum current density on the same heart slice was always smaller than that for a dart between the ribs.

Results of current density on the y axis of the $x = 0$ plane, for the two 0.8 mm diameter dart shapes (sharp and blunt) show that (1) the current density for the blunt dart was higher than the sharp dart, except at the end of the dart; and (2) the difference at the dart tip was about 45%, and when close to the dart it was as large as 26% although it was less than 10% after $y \geq 17$ mm. Thus the sharp dart model was always used. If the heart was 17 mm away from the skin, an approximate shape of the dart (blunt) yielded the correct answer at the heart with less than 9% error.

Figure 5 shows current density contours in the y–z plane at $x = 0$ for a sharp dart as used for the model of a dart inserted between two ribs, for a 1 A inserted current. The internal VF threshold current density values were determined using figure 5 corresponding to the pig VF distances.

For a given VF distance (for example VF skin-to-heart distance $y = 23$ mm) and the corresponding internal current density VF threshold (358 A m^{-2}), the $y = 11$ mm plane had a larger VF threshold current density contour (about 18 mm radius) than the $y = 23$ mm plane (about 1 mm radius).

Figure 6 shows a sample current density contour on the plane of $y = 23$ mm, for 1 A inserted current. If an internal VF threshold current density determined by figure 5 was 358 A m^{-2}, the current density values inside the contour line in figure 6 with that value were greater than 358 A m^{-2}. Therefore the area encircled by that contour line is subject to VF for a dart inserted at the origin ($x = 0$, $z = 0$) of figure 6, for the given VF $y = 23$ mm.

In terms of current density caused at the heart, the dart inserted between the ribs was the most likely to cause VF, followed next by the dart touching ribs, followed then by the Taser electric arc on one node between ribs and the dart on the ribs. The results for the Taser electric arc on one node and the dart on the cartilages were similar. Current density distribution for the dart touching ribs was less than 10% different from current density for the dart between ribs. That was because the dart depth for both cases was the same (9 mm). The bones provided better shields for the current than the cartilages.

The heart ventricles were sliced into surfaces parallel to the skin, with a slice of depth 0 being the slice closest to the skin (figure 7). Since the dart locations most likely to cause VF were aligned with or larger than the heart contours, the

locations closer to the heart were more likely to cause VF except above the sternum (where the dart does not penetrate near the heart). The locations away from ribs were more likely to cause VF than close to ribs. According to our sternum modelling results, darts hitting sternum locations did not cause VF. So the sternum area was subtracted from the dart area most likely to cause VF based on contour results for cartilage ribs to yield the final estimated $A\_y_{sh\_min}\_y_{dh\_VF}$.

person with that skin-to-heart distance is vulnerable to a Taser is listed in column 6. The sum of the products of column 6 with the fraction of such minimum skin-to-heart distances $P\_y_{sh\_min}$ (column 2) was the estimated probability of 0.0000161 for that VF distance data $y_{sh\_VF} = 8$ mm.

Because the minimum human skin-to-heart distance y_{sh_min} from echocardiography data was larger than 9 mm, data for VF distances smaller than 9 mm did not need to be considered.

Mean VF probability for data from a pig when using a blunt probe [10]
$= $ VF probability for VF distance y_{dh_VF} of 2 mm $\times$ fraction of pig VF data at 2 mm
$+$ VF probability for VF distance y_{dh_VF} of 4 mm $\times$ fraction of pig VF data at 4 mm
$+$ VF probability for VF distance y_{dh_VF} of 5 mm $\times$ fraction of pig VF data at 5 mm
$+$ VF probability for VF distance y_{dh_VF} of 6 mm $\times$ fraction of pig VF data at 6 mm
$+$ VF probability for VF distance y_{dh_VF} of 7 mm $\times$ fraction of pig VF data at 7 mm
$+$ VF probability for VF distance y_{dh_VF} of 8 mm $\times$ fraction of pig VF data at 8 mm
$= 0 \times 1/10 + 0.000000235 \times 2/10 + 0.000000817 \times 1/10 + 0.00000264 \times 2/10 + 0.00000688 \times 1/10$
$+ 0.0000161$ (see table 2) $\times 3/10 = 0.000006$.

3.2. Calculating probabilities of VF

In [14] we used table B-5 of [1] to calculate dart hit areas. Later we discovered errors in table B-5 (centre of grid box F = 0.06 from which height F = 0.12, which does not match figure B-1 of [1]). To improve accuracy of this paper we measured distances on figure B-1 of [1]. The probability of a hit in 1 cm^2 frontal chest area by a dart ($P_$hitting $1cm^2\_y_{sh\_min}$, a multiplier in column 6 in tables 2 and 3) varies with the height of the subject with an estimated mean = (probability of hit in frontal chest area)/(area of frontal chest area in cm^2) = [(number of hits in frontal chest area)/(total number of hits)]/(area of frontal chest area in cm^2) = [(373 + 463)/3039]/786.7 = 0.00035. Here 373 and 463 were hit counts from police reports provided in Table B-1 of [1] for grids B3 and C3 on figure B-1. The total number of hits was 3039. The frontal chest area was calculated from the area of grids B3 and C3 on the frontal chest. We used the heights for 150 people in the echocardiography data to scale figure B-1 of [1] and derived the grids area estimated as about 786.7 cm^2. This frontal chest area is smaller than that in [14], which used Table B-5 of [1].

Table 2 shows an example for blunt probe pig data with VF dart-to-heart distance y_{dh_VF} of 8 mm. Several minimum skin-to-heart distances need to be considered. For each minimum skin-to-heart distance y_{sh_min} (column 1), a range of heart slices and electric current density contours for the same heart slice located at skin-to-contour distances y_{sc} (column 3) were considered. The area of the heart slice at depth y_{h_depth} (column 4) can be found from figure 7. The probability that a

Estimated population variance and standard deviation of the VF probability for data from a pig when using a blunt probe were about 0.000000004 and 0.00006.

Similar calculations for resected chest wall pig data yielded mean VF probability of 0.001. Estimated population variance and standard deviation of the VF probability using resected chest wall pig data was about 0.000011 and 0.0034. Details for all dart-to-heart distances are in [14].

In both studies, bootstrap methods yielded approximately the same results of mean and variance. There was very strong evidence against the hypothesis that the VF probability was zero.

The estimated conditional VF probability as a function of dart-to-heart radius (horizontal distance measured parallel to skin surface) both for data from a pig having a resected chest wall and for data from a pig when using a blunt probe are in [14], chapter 4, figures 9–10. It is shown that the VF probability decreases with the dart-to-heart horizontal distance. The dart-to-heart radius most likely to cause VF (the circle within which a dart could cause VF) had a maximum of 53.2 and mean of 7.9 mm for data from a pig having a resected chest wall, and a maximum of 17.3 and mean of 0.18 mm for data from a pig when using a blunt probe. The dart-to-heart radius most likely to cause VF describes a situation where the dart does not land on the sternum.

4. Discussion and conclusions

Recently there has been considerable discussion on the safety of Taser devices [1]. Since Tasers stimulate nerve and

skeletal muscle, they may also stimulate the heart (cardiac muscle) and therefore one possible risk of Taser weapons is that of inducing VF in humans. VF is fatal if not corrected within minutes. Note that the VF mechanism is not completely understood. Only VF caused by electrical stimulation was studied in this paper. This paper only considers one mechanism for induction of VF whereas in fact other mechanisms might be more likely to result in VF in some subjects, e.g. mechanical impact, stress, drug overdose, or spontaneous VF due to heart dysfunction such as coronary artery disease.

The goal of the current study was to estimate the risk of inducing VF in humans by electrical stimulation by Tasers, using computer models in combination with other available data. Our computer modelling results show that current density is very high near the Taser dart, and rapidly decreases with increasing distance from the dart (figure 5). Using previous data on distances between Taser dart and heart at which VF could be induced in pigs, we estimated internal current density VF thresholds for different skin-to-heart distances (figure 5). Depending on how deep the heart is located in a specific person, we estimated the probability of inducing VF after Taser use (see table 2). Combined with data on variability in heart location among humans, we estimated the mean and variance of the total probability of human VF after Taser use, VF probabilities conditioned on dart-to-heart horizontal distance and dart location radii most likely to cause VF for two different pig studies.

The outer skin, fat and muscle layers in the pig study using a blunt dart were not resected. Thus a portion of the current inserted through the 9 mm dart could flow to the outer layers (in the FE model it could not). At a VF distance, the actual VF current density at the heart could be lower than that estimated from the FE model. This could explain the smaller dart-to-heart VF distance and VF probability for data from a pig when using a blunt probe than for data from a pig having a resected chest wall. Nanthakumar *et al*. [7] placed subcutaneous darts parallel to the skin of pigs and administered epinephrine as a continuous intravenous infusion at a dose of 0.1 g kg^{-1} min^{-1} to 0.7 g kg^{-1} min^{-1} titrated to increase the animal's heart rate to a 50% increase from the baseline before discharges. They obtained VF for 1 X26 discharge in 16 for a dart-to-heart distance of about 45 mm. Dennis *et al*. [6] exposed pigs to two prolonged 40-s X26 discharges. They obtained VF for two out of six experimental pigs for a dart-to-heart distance of about 45 mm. Walter *et al*. [8] exposed pigs to two 40-s X26 discharges. They obtained myocardial capture and post-discharge ventricular tachycardia for 1–17 s for all discharges, and VF for one out of eight pigs for a dart-to-heart distance of about 45 mm. For data from a pig having a resected chest wall [9] the average dart-to-heart distance that caused VF was 17 mm. For data from a pig when using a blunt probe [10] the average dart-to heart distance that caused VF was 6.2 mm. While the five studies used different testing techniques, all showed that the probability of VF for some human locations is not zero. The procedures used in the blunt probe study were least disturbing to the pig and hopefully most accurate. In addition to VF probability, we also calculated the radius of the location area where the dart is most likely to cause VF.

The estimated VF probability is contingent on a number of assumptions and limitations from all steps of the whole project: pig experiments, human data measurements, circuit measurements and FE modelling. Each known or unknown factor could contribute to the deviation of the estimation away from the true value. For example:

(1) It was assumed that all darts were perpendicular to the skin. Those darts with nonperpendicular angles had a penetration depth of less than 9 mm.
(2) Our FE model used one centred dart surrounded by grounding. The results may be slightly different using two darts on a full torso model.
(3) The internal VF thresholds used FE models with a sharp dart only.
(4) It was assumed that all darts were on bare skin. If clothing were present, the arc may jump to the skin but the penetration depth would be less than 9 mm.
(5) Our FE model used isotropic electric conductivities. At Taser frequencies, intercostal skeletal muscles have a small anisotropy.
(6) Isoflurane anaesthesia used during the pig studies alters the VF induction in the pig, and increases the VF threshold [21].
(7) VF induction in the human may differ from that in the pig.
(8) Lungs were not considered.
(9) The human subjects in the echocardiography data may not resemble the usual Taser subjects.
(10) The model simplification process tended to consider the worst case and tended to estimate a probability higher than without the simplification. But the estimated mean VF probability could not be claimed as an upper bound for the true probabilty because there are unclear effects of many other factors besides FE modelling, known or unknown.

Most of the assumptions would cause only a small change in the result.

Predicting the likelihood of rare events is highly uncertain in general. The Taser causing direct VF is a rare event, and thus is difficult to estimate. There are many uncertainties in the animal tests and the computer modelling. Thus these results are a best estimate that provides an order of magnitude of the probability of this rare event.

The presented results may help to determine appropriateness of use for Tasers when apprehending offenders. The dart-to-heart distances most likely to cause VF on the skin plane (radius) were small (up to about 53 mm for resected chest wall data). VF need not be fatal. It can be reversed if a defibrillator is used within minutes. Myerburg *et al*. [22] suggested that a defibrillator is carried in police cars.

Necessary, but not sufficient, conditions for direct electrocution of the heart by the Taser are (1) dart landing in a frontal region near the heart suggested by our results and results of others, and (2) cardiac arrest of the subject shortly after Taser firing suggested by the literature. Coroners should seek to confirm these conditions before ascribing Tasers as a contributing cause of death. These results suggest that during police training Taser darts landing on the back of the torso are less likely to cause VF than darts landing on the front because the back is farther from the heart. For any electromuscular incapacitating device that has (1) a pulse duration much shorter than the time constant for cardiac excitation of about 2 ms, (2) low duty cycles, and (3) a dart 9 mm long and 0.8 mm in diameter, these results would be transferable by using the strength–duration curve [11]. A standard for Tasers has been proposed [23].

This is the first study that provides a positive numerical estimate of the probability that Tasers can cause VF in humans.

Acknowledgments

This project was supported by Grant No. 2004-IJ-CX-K036 awarded by the National Institute of Justice, Office of Justice Programs, US Department of Justice. Points of view in this document are those of the authors and do not necessarily represent the official position or policies of the US Department of Justice.

References

[1] Maier, A., Nance, P., Price, P., Sherry, C.J., Reilly, J.P., Klauenberg, B.J. and Drummond, J.T. 2005, *Human Effectiveness and Risk Characterization of the Electromuscular Incapacitation Device—A Limited Analysis of the TASER. Part II – Appendices* (The Joint Non-Lethal Weapons Human Effects Center of Excellence), 1 March 2005. Accessed 26 Dec 09 at new location http://ccvweb.csres.utexas.edu/collections/papers/ccvmaya/Papers/zhang-1721_heart.pdf. Available online at: http://www2.taser.com/research/Science/Documents/The%20Joint%20Non-Lethal%20Weapons%20Human%20Effects%20Center%20of%20Excellence%20Part%20II.pdf.

[2] Geddes, L.A., 2004, The small heart and the critical mass for ventricular fibrillation. *IEEE Engineering in Medicine and Biology Magazine*, **23,** 196–197.

[3] Malkin, R.A., Eynard, J.N. and Pergola, N.F., 1997, Extended cardiac tachyarrhythmias in guinea pigs. *Proceedings of the International Conference of the IEEE Engineering in Medicine and Biology Society,* 387–388.

[4] Malkin, R.A. and de-J Curry, A., 2003, Frequency dependence of the cardiac threshold to alternating current between 10 Hz and 160 Hz. *Medical & Biological Engineering & Computing*, **41,** 640–645.

[5] Holden, S.J., Sheridan, R.D., Coffey, T.J., Scaramuzza, R.A. and Diamantopoulos, P. 2007, Electromagnetic modelling of current flow in the heart from TASER devices and the risk of cardiac dysrhythmias. *Physics in Medicine and Biology*, **52,** 7193–7209.

[6] Dennis, A.J., Valentino, D.J., Walter, R.J., Nagy, K.K., Winners, J., Bokhari, F., Wiley, D.E., Joseph, K.T. and Roberts, R.R. 2007, Acute effects of TASER X26 discharges in a swine model. *Journal of Trauma*, **63,** 581–590.

[7] Nanthakumar, K., Billingsley, I.M., Masse, S., Dorian, P., Cameron, D., Chauhan, V.S., Downar, E. and Sevaptsidia, E. 2006, Cardiac electrophysiological consequences of neuromuscular incapacitating device discharges. *Journal of the American College of Cardiology*, **48,** 798–804.

[8] Walter, R.J., Dennis, A.J., Valentino, D.J., Margeta, B., Nagy, K.K., Bokhari, F., Wiley, D.E., Joseph, K.T. and Roberts, R.R. 2008, TASER X26 discharges in swine produce potentially fatal ventricular arrhythmias. *Academic Emergency Medicine*, **15,** 66–73.

[9] Wu, J.-Y., Sun, H., O'Rourke, A.P., Huebner, S., Rahko, P.S., Will, J.A. and Webster, J.G. 2007, Taser dart-to-heart distance that causes ventricular fibrillation in pigs. *IEEE Transactions on Biomedical Engineering*, **54,** 503–508.

[10] Wu, J.-Y., Sun, H., O'Rourke, A.P., Huebner, S., Rahko, P.S., Will, J.A. and Webster, J.G. 2008, Taser blunt probe dart-to-heart distance causing ventricular fibrillation in pigs. *IEEE Transactions on Biomedical Engineering*, **55,** 2768–2771.

[11] Geddes, L.A. and Baker, L.E., 1989, *Principles of Applied Biomedical Instrumentation,* 3rd edn (New York: John Wiley & Sons).

[12] MacLeod, R.S., Johnson, C.R. and Ershler, P.R., 1991, Construction of an inhomogeneous model of the human torso for use in computational electrocardiography. *Proceedings of the 13th Annual International Conference of the IEEE Engineering in Medicine and Biology Society*, **13,** 688–689.

[13] Zhang, Y. and Bajaj, C., 2004, Finite element meshing for cardiac analysis. *ICES Technical Report 04-26*. The University of Texas at Austin. Available online at: http://www.ices.utexas.edu/~jessica/medical_data/heart/Heart_Valve_new.htm.

[14] Sun, H., 2007, Models of ventricular fibrillation probability and neuromuscular stimulation after Taser® use in humans. *Ph.D. thesis,* University of Wisconsin. Available online at: http://ecow.engr.wisc.edu/cgi-bin/get/bme/762/webster/sun-thesis-01-21-07.pdf.

[15] Cormier, J.M., 2003, Microstructural and mechanical properties of human ribs. *M.Sc. Thesis,* Department of Mechanical Engineering, Virginia Polytechnic Institute and State University.

[16] Dahiphale, V.P., Baheete, B.H. and Kamkhedkar, S.G., 2002, Sexing the human sternum in Marathwada region. *Journal of Anatomical Society of India*, **51,** 162–167. Available online at: http://medind.nic.in/jae/t02/i2/jaet02i2p162.pdf.

[17] Casha, A.R., Gauci, M., Yang, L., Saleh, M., Kay, P.H. and Cooper, G.J. 2001, Fatigue testing median sternotomy closures. *European Journal of Cardiothoracic Surgery*, **19,** 249–253. Available online at: http://ejcts.ctsnetjournals.org/cgi/ijlink?linkType=ABST&journalCode=ejcts&resid=19/3/249.

[18] Gabriel, C., Gabriel, S. and Corthout, E., 1996, The dielectric properties of biological tissues: I. Literature survey. *Physics in Medicine and Biology*, **41,** 2231–2249. Available online at: http://niremf.ifac.cnr.it/tissprop/.

[19] Rahko, P.S. 2008, Evaluation of the skin-to-heart distance in the standing adult by two-dimensional echocardiography. *Journal of the American Society of Echocardiography*, **21,** 761–764.

[20] Gray, H., 1977, T. Pickering Pick and R. Howden (Eds.) *Anatomy, Descriptive and Surgical,* revised 15th edn (New York: Gramercy, To: Gray, H., T.P. Pick and R. Howden (Eds.) 2007, Anatomy, Descriptive and Surgical (Raleigh, NC: Sweetwater Press).

[21] Pagel, P.S., Kersten, J.R., Farber, N.E., Waltier, D.C. 2005, Cardiovascular pharmacology. In: R.D. Miller (Ed.) *Miller's Anesthesia,* 6th edn, Chapter 7 (Philadelphia, PA: Elsevier Churchill Livingstone), pp. 191–229.

[22] Myerburg, R.J., Fenster, J., Velez, M., Rosenberg, D., Lai, S., Kurlansky, P., Newton, S., Knox, M. and Castellanos, A. 2002, Impact of community-wide police car deployment of automated external defibrillators on survival from out-of-hospital cardiac arrest. *Circulation*, **106,** 1058–1064.

[23] Nimunkar, A.J. and Webster J.G. 2009, Safety of pulsed electric devices. *Physiological Measurement*, **30,** 101–114.